Inkjet and inkjet-based 3D printing: connecting fluid properties and printing performance

Yang Guo, Huseini S. Patanwala and Brice Bognet
Institute of Materials Science, University of Connecticut, Storrs, Connecticut, USA, and
Anson W.K. Ma
Polymer Program, Institute of Materials Science, University of Connecticut, Storrs, Connecticut, USA and
Department of Chemical and Biomolecular Engineering, University of Connecticut, Storrs, Connecticut, USA

Abstract

Purpose – This paper aims to summarize the latest developments both in terms of theoretical understanding and experimental techniques related to inkjet fluids. The purpose is to provide practitioners a self-contained review of how the performance of inkjet and inkjet-based three-dimensional (3D) printing is fundamentally influenced by the properties of inkjet fluids.

Design/methodology/approach – This paper is written for practitioners who may not be familiar with the underlying physics of inkjet printing. The paper thus begins with a brief review of basic concepts in inkjet fluid characterization and the relevant dimensionless groups. Then, how drop impact and contact angle affect the footprint and resolution of inkjet printing is reviewed, especially onto powder and fabrics that are relevant to 3D printing and flexible electronics applications. A future outlook is given at the end of this review paper.

Findings – The jettability of Newtonian fluids is well-studied and has been generalized using a dimensionless Ohnesorge number. However, the inclusion of various functional materials may modify the ink fluid properties, leading to non-Newtonian behavior, such as shear thinning and elasticity. This paper discusses the current understanding of common inkjet fluids, such as particle suspensions, shear-thinning fluids and viscoelastic fluids.

Originality/value – A number of excellent review papers on the applications of inkjet and inkjet-based 3D printing already exist. This paper focuses on highlighting the current scientific understanding and possible future directions.

Keywords Review, Rheology, 3D printing, Inkjet printing, Surface science

Paper type Literature review

1. Introduction

Inkjet printing has been widely adopted, as the technology was first developed in the 1960s to 1970s (Buehner *et al.*, 1977; Elmqvist, 1951; Sweet, 1965, 1975; Vaught *et al.*, 1984). Presently, inkjet printing has evolved from applications such as product coding and graphic art printing to more advanced applications such as digital fabrication and additive manufacturing. As shown in Figure 1, the number of journal articles published on inkjet printing has grown steadily since early 2000s, with a lot of patent activities occurring between 2004 and 2007. Inkjet printing has a number of technical advantages, making it an attractive method for manufacturing. First, inkjet printing is a non-contact method. It is scalable and is less susceptible to contamination and substrate or mask damage. Second, inkjet printing is a digital process offering great versatility in terms of patterning through drop deposition. It has been applied to create three-dimensional (3D) structures layer-by-layer by printing a binder onto a powder bed or jetting a photopolymer which is subsequently cross-linked (Sachs *et al.*, 1992; Wang *et al.*, 2008). Third, inkjet printing is compatible with different fluids including polymer solutions, particle suspensions and biomolecules provided that the "ink" satisfies certain fluid requirements. Table I summarizes some common types of inkjet fluids and their applications.

1.1 Printing process overview

The two main modes of inkjet printing are continuous inkjet (CIJ) mode and drop-on-demand (DOD) mode, as illustrated in Figure 2(a) and (b). In both methods, the liquid goes through an orifice or nozzle. In the CIJ mode, as its name suggests, the fluid is pushed through the nozzle continuously. The jet then breaks into a stream of droplets as a result of capillary-driven Rayleigh-Plateau instability. Droplets are charged and deflected using field plates onto the substrate during printing, while the rest are collected by a catcher for recycling. CIJ typically produces a high drop velocity (>10 ms^{-1}) (Derby, 2010) and thus enables fast

The current issue and full text archive of this journal is available on Emerald Insight at: **www.emeraldinsight.com/1355-2546.htm**

Rapid Prototyping Journal
23/3 (2017) 562–576

[DOI 10.1108/RPJ-05-2016-0076]

The authors would like to acknowledge the Faculty Large Grant at the University of Connecticut for financial support.

Received 5 May 2016
Revised 21 June 2016
Accepted 24 June 2016

Figure 1 (a) Number of new journal articles published from 1973 to 2015, data collected using Scopus with "inkjet" as the search keyword; (b) number of new patents from 1973 to 2015, data collected using LexisNexis with "inkjet" as the search keyword

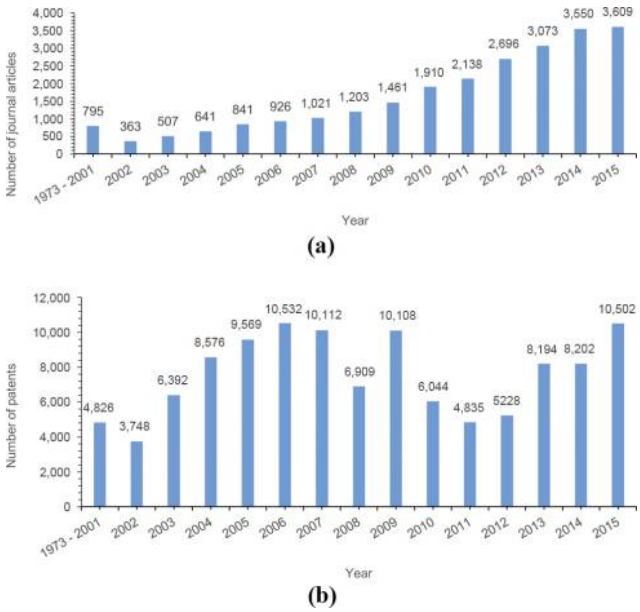

processing for applications such as marking and bar coding. Due to the continuous jetting action, the nozzle is less likely to be clogged due to solvent evaporation especially if a volatile solvent is used. However, the resolution of CIJ is generally lower than that of DOD (Hutchings and Martin, 2012). Also, the deposition of small fragmented drops onto the field plates can modify the electric field and in worst cases can lead to printer failure. Recycling of the ink may also lead to contamination and require re-adjusting the ink concentration to account for solvent evaporation. DOD-type inkjet printing is more widely used, where the drop is only generated as needed by thermal or piezoelectric actuation. The typical drop velocity is around 5 to 8 m s^{-1} (Hutchings and Martin, 2012). A drawback of DOD printing is the drying of ink at the nozzle during downtime, which may further lead to particulate deposition at the nozzle and possible clogging.

Several 3D printing methods are based on inkjet technology. For instance, in the 3DP™ powder-bed method licensed by MIT, a binder is printed onto a powder bed. As illustrated in Figure 2(c), the binder material selectively consolidates the powder, thereby forming a quasi-2D pattern. The fused layer is then lowered into the powder bed, and another layer of powder is smoothly spread onto the surface by a roller, followed by another round of binder printing. By repeating this process, 3D structures can be fabricated (Sachs *et al.*, 1993). Such method has been applied to create ceramic-based polymer composites (Seerden *et al.*, 2001) and intricate candies (von Hasseln, 2013). More recently, one of the licensees, Aprecia Pharmaceuticals, has applied the 3DP™ method to create FDA-approved fast-dissolving tablets (Katstra *et al.*, 2000; Rowe *et al.*, 2000). Process development steps from powder and binder selection to post-processing for 3DP™ are reviewed by Utela *et al.* (2008). Another inkjet-based 3D printing method involves printing photopolymers and support materials layer-by-layer, where the water-soluble support material will be subsequently removed.

1.2 Printing performance parameters

Regardless of the method, the printing performance is evaluated in terms of the resolution, consistency and drop placement accuracy. Dots per inch (DPI) is commonly used as a measure of printing resolution, which accounts for the distance between two adjacent droplets deposited on the substrate, depending on the incremental X and Y displacements of the print head or substrate. However, the resolution also depends on the actual footprint of the deposited drops, which is not specified in DPI. For DOD inkjet printing, the spatial resolution is typically on the order of tens of microns (Hutchings and Martin, 2012). The footprint of a drop further depends on the drop volume and the contact angle between the drop and the substrate.

Table I Common materials and application examples of inkjet printing and inkjet-based 3D printing

Category	Sample materials	Application examples
Polymers, monomers and oligomers	Conjugated polymers [e.g. poly(3,4-ethylenedioxythiophene), poly(pyrrole), polyaniline, and poly(p-phenylene vinylene)]	Transistors (Sirringhaus, Kawase *et al.*, 2000), displays (Shimoda *et al.*, 2003), polymer light-emitting devices (PLED) (Bharathan and Yang, 1998), sensors (Crowley *et al.*, 2008; Dua *et al.*, 2010), solar cells (Chen *et al.*, 2009), 3D structures (van den Berg *et al.*, 2007), radio-frequency identification (RFID) (Rida *et al.*, 2009; Yang *et al.*, 2007), and flexible electronics (Perelaer *et al.*, 2006)
Metal and metal oxide, carbon materials	Silver and gold nanoparticle dispersions; Silver and gold precursor solutions; Graphene, carbon nanotubes and carbon black	
Ceramic	Alumina, zinc oxide and silicon nitride/oxide	Capacitors, 3D structures (Cappi *et al.*, 2008; Seerden *et al.*, 2001)
Biomaterials	Biomolecules (e.g. proteins and DNA) and cells	Biochips, biomarkers (Delaney *et al.*, 2009; Okamoto *et al.*, 2000), biosensors and immunoassay tests (Delaney *et al.*, 2009), and regenerative medicine (Calvert, 2007; Lorber *et al.*, 2014; Murphy and Atala, 2014)

Figure 2 (a) Basic principles of CIJ; (b) DOD printers (Martin *et al.*, 2008); (c) process diagram of powder-bed based 3D printing, where a binder is jetted onto a powder bed to create 3D objects (Sachs *et al.*, 1993)

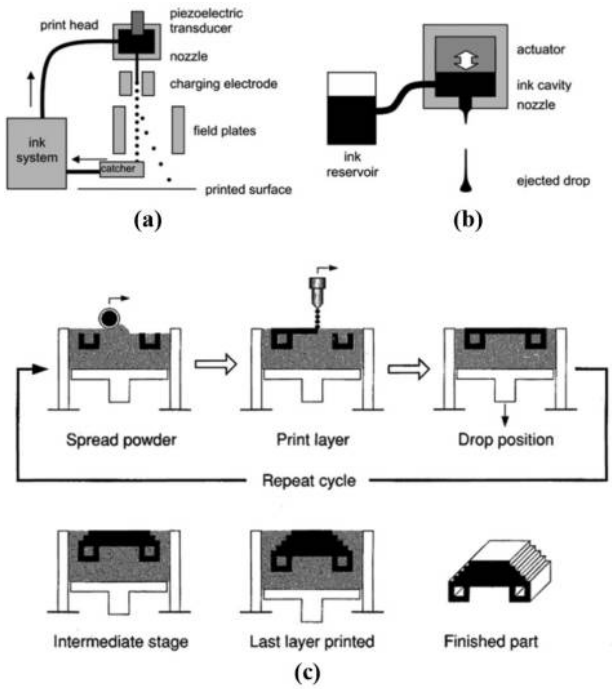

Source: Reprinted with permission from Elsevier

Consistency is especially important for large-scale manufacturing. Inconsistency due to misfiring, nozzle-plate flooding and satellite drop formation are closely related to the fluid properties, namely, rheology and surface tension, of the ink. Drop placement error is defined as the difference between the target location and the impact location (Lean, 2002). The error is influenced by the precision of the nozzle manufacturing and the distance between the nozzle and substrate. In high throughput systems, the substrate moves at a high speed (e.g. Kodak Inkjet printer Versamark® Series can go up to 1,000 feet/min). Positioning smaller drops becomes increasingly difficult as a boundary layer is developed immediately above the surface of moving substrate, which may deflect the drops and, in some cases, prevent the small drops from reaching the substrate surface entirely (Leoni and Gila, 2013).

1.3 Review scope and structure

This paper summarizes the latest developments both in terms of theoretical understanding and experimental techniques related to inkjet fluids. This review paper is written with practitioners in mind, who may not be familiar with the underlying physics of inkjet printing. For this reason, the paper starts with a brief review of basic concepts in inkjet fluid characterization and the relevant dimensionless groups for describing the inkjet printing process. To further connect the printing performance with the fundamental understanding, we discussed three types of commonly used inkjet fluids, namely, particle suspensions, shear-thinning fluids and viscoelastic fluids. These inkjet fluids are "complex fluids" that possess mechanical properties that are intermediate between ordinary liquids and ordinary solids" (Gelbart and Ben-Shaul, 1996; Larson, 1999). Additionally, we also review how drop impact and contact angle affect the footprint and resolution of inkjet printing. Of particular interest are drop spreading and infiltration for powder and fabrics that are technologically important for 3D printing and smart clothing. Finally, a future outlook is given at the end of this review paper, highlighting technological gaps and possible future research directions. All in all, this paper aims to provide practitioners a self-contained review without duplicating excellent existing reviews on the jetting of Newtonian fluids and inkjet printing (Derby, 2010; Eggers and Villermaux, 2008; Martin *et al.*, 2008). This review paper focuses on inkjet-based 3D printing methods (e.g. 3DP^{TM}) only. There is a vast literature on other types of 3D printing methods, such as fused deposition modeling (FDM), stereolithography and selective laser sintering. Interested readers are referred to Dimitrov *et al.* (2006), Espalin *et al.* (2014), Gibson *et al.* (2015), Melchels *et al.* (2010), Murphy and Atala (2014), Sachs *et al.* (1997), Turner and Gold (2015), Upcraft and Fletcher (2003) and Yan and Gu (1996).

2. Ink characterization: viscosity and surface tension

2.1 Surface tension measurement

The density (ρ), surface tension (σ) and the viscosity (η) of the fluids are physical properties that are relevant to inkjet printing. Surface tension originates from the cohesive forces experienced by the molecules at the surface of a liquid. A number of techniques can be used to measure the surface tension of a liquid. A detailed review of each experimental technique is beyond the scope of this paper, and interested readers should refer to Adamson (1990). We will only highlight three commonly used methods, namely, Wilhelmy plate, du Noüy ring and pendant drop methods. In the Wilhelmy plate method, a plate, usually made of surface-treated platinum or paper, is inserted into a fluid of interest. As the fluid wets the plate, the plate experiences a downward wetting force. The net force applied on the plate can be expressed as: $F = W_p + 2(d + w)\gamma cos\theta$, where F is the force applied to the plate, W_p is the weight of the plate, d is the thickness of the plate, w is the width of the plate, γ is the surface tension of the liquid and θ is the contact angle. If the plate is completely wetted by the liquid, $cos\theta = 1$. By measuring the force using a microbalance, the surface tension can be calculated. In the du Noüy ring method, a platinum ring instead of a plate is submerged in the liquid. The ring is attached to a microbalance that measures the force as the ring is pulled out of the liquid. The interfacial tension can be calculated from the following equation $F = W_r + 4\pi R\gamma$, where W_r is the weight of the ring, R is the radius of the ring (inner diameter is assumed to be the same as the outer diameter because the ring is designed to be thin) and γ is the surface tension. In the pendant drop method, a drop is dispensed at the tip of a syringe needle. As drop volume increases, the drop shape is progressively distorted from a spherical shape due to gravity. The exact shape of the drop is described by the Bashforth and Adams (1883) equation, which

considers the competition between capillary and gravitational forces. The surface tension of the fluid is calculated by imaging the drop using a camera and fitting the drop shape (Maze and Burnet, 1971). It is worth noting that Wilhelmy plate and du Noüy ring methods are commonly used to measure the equilibrium surface tension, whereas the pendant drop method may be used to measure dynamic surface tension of drops containing surface active molecules, for example (Hoath *et al.*, 2012; Morita *et al.*, 2010). However, the time scale associated with such method is in excess of 0.01 s, orders of magnitude larger than that experienced during inkjet printing, which is on the order of microseconds.

2.2 Rheological characterization

The apparent shear viscosity of a fluid represents the fluid's resistance towards flow and is defined as the shear stress divided by the shear rate. The viscosity of a Newtonian fluid is independent of the shear rate, but in general the viscosity of a fluid may depend on the shear rate applied. Shear-thinning fluids are fluids of which the apparent viscosity decreases as the shear rate increases. Conversely, shear-thickening fluids are fluids of which the apparent viscosity increases as the shear rate increases. In inkjet printing, the printing fluid is subjected to high shear rates, typically in excess of 10^4 s^{-1} (Reis *et al.*, 2005), and a short residence time on the order of 5 – 250 μs (Hutchings and Martin, 2012). In addition to shear-rate dependence, a fluid may also exhibit viscoelasticity, where the stress is proportional to the strain rate as well as the strain. For instance, the addition of colloidal particles and polymers may result in elasticity (Hoath *et al.*, 2014; Wagner and Brady, 2009).

The viscoelastic response of a fluid depends on the characteristic time scale of the process relative to the characteristic time scale of the fluid. In piezoelectric-based inkjet print heads, the printing fluids are subjected to frequencies on the order of 10-100 kHz (de Jong *et al.*, 2006). Measuring the flow behavior, or rheology, of printing fluids at these relevant time scale and frequencies is important for correlating the basic rheology to their actual behavior during the printing process. Commercial torsional rheometers may be used to characterize the basic rheology of the printing fluids; however, the highest accessible shear rates and frequencies are limited by the motor response and inertia and are typically orders of magnitude lower than those relevant to inkjet printing. Capillary rheometers are capable of measuring the fluid viscosity at high shear rates, but the corresponding residence time is on the order of milliseconds – much longer than that experienced by the printing fluid (approximately 10 μs) (Wang *et al.*, 2012).

As for high-frequency rheology, a custom-built squeeze-flow rheometer, named piezo-axial vibrator (PAV), has been developed by Pechhold *et al.* at the University of Ulm (Kirschenmann and Pechhold, 2002). The PAV is driven by a piezoelectric element and can access a frequency ranging from 1 Hz up to 12 kHz, closer to the characteristic frequencies relevant to inkjet printing. Torsional resonators, first explored by Mason (1947), are able to achieve to megahertz regime, but mostly limited to a single frequency (Mason, 1947). Wagner and co-workers developed a set of two torsional resonators which provides access to five discrete frequencies between 3.7 and 57 kHz (Fritz *et al.*, 2003).

2.3 Direct imaging

Given the challenges in measuring the rheology at high frequencies, short residence time and high shear rates, direct imaging of the jetting behavior proves to be a more straightforward method to evaluate the jettability of printing fluids. Both the spatial resolution and temporal resolution of the imaging method are important for getting high-quality, sharp images for quantitative analysis. A detailed review on high-speed imaging of fluids is published elsewhere (Versluis, 2013). A typical imaging platform involves a camera, a light source, a print head with control unit and trigger control to synchronize the jetting and the imaging. The key is to reduce the effective exposure time, which depends on both shutter speed and the illumination conditions. Small exposure time may be achieved using a high-speed camera and/or a strobe light source. The shutter speed of the camera and the brightness of the light source affect the image quality obtained from high-speed cameras.

Although the frame rate of high-speed cameras is typically in excess of thousands, the corresponding exposure time is on the order of milliseconds or less, which is longer than the illumination time of a flash light source on the order of nanoseconds. Besides, spatial resolution is compromised as the frame rate increases as the number of frames is limited by the data transfer speed. Several research groups have applied high-speed and stroboscopic imaging to capture the drop formation in inkjet printing (Dong *et al.*, 2006; Hutching *et al.*, 2007). For instance, Hutching *et al.* (2007) used a high-speed camera with a "spark flash" light source with an intense 20-ns illumination to reduce the image blurring of drops traveling at a speed of 5 to 20 m/s. Figure 3 compares the image collected using the spark flash technique with that captured with an ordinary strobe light. Technological advances in LED lighting

Figure 3 Images of a UV-curable ink jetted into air captured using: (a) a standard strobe illumination with longer illumination time (≥1 μs); and (b) a "spark flash" technique with 20-ns flash illumination (Hutching *et al.*, 2007)

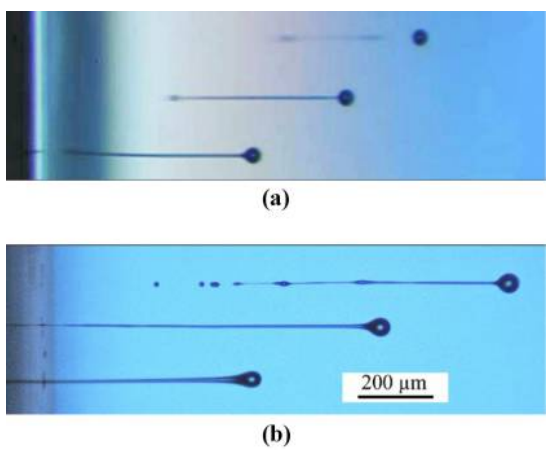

Source: Reprinted with permission of IS&T: The Society for Imaging Science and Technology sole copyright owners of *Journal of Imaging Science*

have enabled the development of inkjet imaging platforms at a relatively low cost. Further, Bognet *et al.* (2016) developed an inkjet fluid testing platform using inexpensive sound card, instead of a lock-in amplifier, to synchronize the jet actuation and imaging with a time precision of 5 μs.

2.4 Dynamic measurements

Dynamic surface tension and viscosity data may be obtained by directly imaging and recording the oscillations of a free-flight drop. In general, Newtonian fluids follow a "free shape" mode, where the restoration of drop shape and damping of oscillations are due to the surface tension and viscosity (Lamb, 1895). Recent studies suggested that such analysis may be extended to complex fluids. Yang *et al.* reported dynamic surface tension data for drops with a volume in the pL to μL range and for an experimental time scale of 10^{-5} to 10^{-2} s. In this work, drop oscillating method was first validated by using hydroxyethyl cellulose aqueous solutions and further applied to aqueous poly (3,4-ethylenedioxythiophene) polystyrene sulfonate (PEDOT:PSS) solutions and colloidal suspensions, which are shear thinning (Yang *et al.*, 2014). Hoath *et al.* studied oscillating drops of aqueous solutions containing PEDOT:PSS, which exhibited shear-thinning behavior. The viscosity of PEDOT:PSS solution first decreased as the droplet exited the nozzle due to high shear, but the viscosity subsequently increased as the drop detached from the nozzle. Additionally, the dynamic surface tension values were also found to be 1.5 to 2 times higher than the equilibrium values because of the finite time scale (approximately 4 ms) for the surface active molecules to diffuse from the bulk to the interface (Hoath *et al.*, 2015). The free-flight drop analysis offers important access to fluid properties at a time scale that is relevant to inkjet printing.

3. Jet breakup and drop formation

The jet breakup and drop formation during inkjet printing depends on the interplay between inertial, viscous, elastic and surface forces. Table II summarizes the dimensionless numbers that are useful for understanding the jetting behavior and identifying the printable region [Figure 4(a)]. The magnitude of dimensionless numbers indicates the relative importance of different forces and time scales at play, as described in greater detail in Table II. For a simple Newtonian fluid where the viscosity is independent of the shear rate and there is no elasticity, the Ohnesorge number can be used to determine a range in which printing is possible. Derby (2010, 2011) found that if the Oh number is too large (>1), the fluid is so viscous that there is not sufficient energy to form a jet and that if the Oh number is too small (<0.1), surface tension will induce satellite drop formation. The Oh number of the printable region is estimated to be between 0.1 and 1, as illustrated in Figure 4(a). For fluid mixtures of ethanol, water and ethylene glycol, the printable region was determined experimentally to be between an Oh-value of 0.07 to 0.25 (Jang *et al.*, 2009).

While calculating the Oh number may be useful, the prediction of the printable region is based on a simple Newtonian fluid. Additional dimensionless groups, such as the Weissenberg (Wi) number and Deborah (De) number, are needed for describing the behavior of viscoelastic fluids. The product of Wi and De numbers results in a dimensionless "Elasticity number" (El), which describes the relative importance of the inertia and elastic stresses (McKinley, 2005). The proper use of Wi and De numbers requires correctly identifying the characteristic time of the fluid, the characteristic time of the deformation and the time of observation. Identifying a single, appropriate characteristic time for the fluid is challenging in practice because most complex fluids have multiple relaxation times. In such cases, the characteristic time of the fluid is taken as either the first moment of the relaxation times or the longest relaxation time (Dealy, 2010). Clasen *et al.* (2012) studied the dispensing of model Newtonian, shear thinning and viscoelastic fluids and demonstrated how different dimensionless groups can be practically used to map out an operating space for dispensing complex fluids. They observed that material-property-based dimensionless groups (Oh, De and Ec) define which mechanism (inertial, viscosity and elasticity) dominates the initial filament thinning process, whereas dynamic (i.e. jet-velocity-dependent) dimensionless groups (Ca, We and Wi) determine the dominant mechanism (dripping vs jetting) during the subsequent thinning [Figure 4(b)]. The authors put forward several theoretical transition values. For instance, if Oh > 0.2077, viscous effects dominate inertia, and if Ec > 4.7015, elastic effects dominate viscous effects. Likewise, if De > 0.9766, elastic effects dominate inertia. The six dimensionless groups are interrelated. A set of

Table II Typical dimensionless groups used to describe capillary thinning and jetting of Newtonian and viscoelastic fluids

Dimensionless group	Definition	Physical meaning
Ohnesorge number	$Oh = We^{1/2}/Re$	Relative importance of viscous compared to inertia and surface forces
Deborah number	$De = \lambda/\sqrt{\rho R^3/\sigma}$	Ratio between the elastic relaxation time and the time of observation (or the capillary thinning time scale)
Elasto-capillary number	$Ec = \lambda\sigma/\eta R$	Relative importance of elastic and capillary effects compared to viscous effects
Weber number	$We = \rho DV^2/\sigma$	Ratio between inertia and surface forces
Weissenberg number	$Wi = \lambda V/D$	Ratio between the characteristic relaxation time of the fluid and deformation rate
Capillary number	$Ca = \eta V/\sigma$	Relative importance of viscous forces and surface tension
Elasticity number	$El = Wi/Re = \eta\lambda/\rho D^2$	Relative importance of inertia and elastic forces
Reynolds number	$Re = \rho DV/\eta$	Ratio between inertia and viscous forces

Notes: ρ is the density, η is the viscosity, σ is the surface tension and λ is the characteristic time of the fluid, whereas D is the characteristic length (usually the nozzle diameter) and V is the velocity of the jet

Figure 4 (a) Printable region identified for simple Newtonian fluids based on the dimensionless Weber number, Reynolds number and Ohnesorge number (Derby, 2011). Reprinted with permission from Elsevier; (b) operating space defined by dimensionless groups for dispersing complex fluids (Clasen *et al.*, 2012). Reprinted with permission from John Wiley & Sons

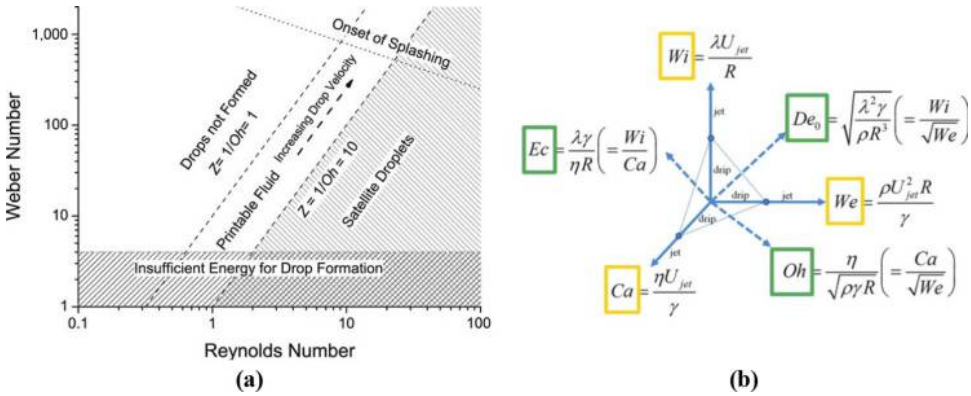

two material-property-based dimensionless groups and one dynamic group are required to fully describe a dispensing operation. Further, the dominant mechanism may change during the thinning process. To account for this, the authors proposed to define the dimensionless groups using the time-dependent filament radius instead (Clasen *et al.*, 2012). In the next section, the current understanding of three different common types of inks, namely, particle suspensions, viscoelastic fluids and phase-change fluids, will be presented.

4. Common inkjet fluids

4.1 Particle suspensions

In graphic art printing, pigments are used to create colors, where the insoluble pigments are first dispersed in a fluid, forming a suspension. The use of pigment suspensions for inkjet printing can be traced back to 1970s (Buehner *et al.*, 1977). More recently, suspensions containing metal- and carbon-based particles are used to create conductive patterns and antennas on substrates for electronic applications (Rida *et al.*, 2009; Singh *et al.*, 2010; Tortorich and Choi, 2013). The stability of the suspension-based inks over time is an important parameter for ink formulations, as it determines the shelf lives of the inks. Particles may settle due to gravity and density difference between the particles and suspending medium. The settling velocity may be estimated using the Stokes equation:

$$V_{settle} = \frac{2}{9}\frac{(\rho_p - \rho_f)}{\eta} g R_p^2 \quad (1)$$

where V_{settle} is the settling velocity (m/s), g is the gravity constant (m/s^2), ρ_p and ρ_f are the densities of the particle and the fluid, respectively (kg/m^3), R_p is the radius of the particle (m) and η is the dynamic viscosity (Pa s).

Although equation (1) suggests that the settling velocity decreases with reducing particle sizes, it does not account for the increase in the surface energies of the systems associated with small particles like nanoparticles, which will likely lead to particle aggregation and consequently sedimentation and probable nozzle clogging. In such cases, polymers and/or surfactants are usually added to stabilize the suspension by inducing electrostatic interactions and steric hindrance. As a rule of thumb, the effective size of the particles should be 20 to 50 times less than the nozzle diameter to avoid clogging (Hutchings and Martin, 2012). For particles with a high tendency to settle, a print head with recirculation may be used to keep the particles suspended (Riegger *et al.*, 2014).

4.1.1 Rheology of particle suspensions

The rheology of a particle-based ink depends on the loading of the particles. Inclusion of particles in a liquid is known to increase the viscosity of the suspension (Einstein, 1906, 1911; Larson, 1999). However, at low particle concentrations, the ink behaves essentially like the suspending medium, as a low-viscosity fluid. Derby (2011) plotted Z (= 1/Oh) values based on the experimental data of ceramic suspensions from literature and found that the printable region shows a good agreement with Reis's theoretical prediction ($1 < Z < 10$). Reis *et al.* (2005) studied concentrated (20 to 40 vol.%) suspensions of fine, dispersant-stabilized alumina particles (0.3 μm) using a piezoelectric drop generator. They observed a linear dependence of both the drop velocity and volume on the driving voltage and a periodic dependence on the frequency and pulse period. The authors suggested the periodic behavior is a result of the acoustic properties of the chamber.

Wang *et al.* (2012) matched the low-shear viscosity of a Newtonian fluid and two particle suspensions. They noted that achieving consistent jetting is more difficult for the particle suspensions. As shown in Figure 5(a), the viscosity of both particle suspensions decreases as a function of increasing shear rate, termed "shear thinning". For highly concentrated suspensions, an opposite "shear thickening" effect may occur (Wagner and Brady, 2009). However, such effect is rarely observed for suspensions used in inkjet printing, where the particle loading is typically less than 20 per cent by volume to maintain a sufficiently low viscosity for printing.

4.1.2 Two-stage breakup process

Furbank and Morris (2004) studied the effects of particles on drop formation using a stroboscopic imaging platform. At low particle concentrations with a volume fraction less than 0.1, suspensions showed a pinch-off structure similar to that exhibited by a pure liquid as the diameter of the liquid thread decreased due to surface tension. However, particles may be trapped within the liquid thread, leading to the formation of

Figure 5 (a) Shear viscosity data of pigment (0, 5.7 and 15 per cent; CAB-O-JET 200®, Cabot Corp.) in a Newtonian liquid mixture of water and glycerin, measured using a Couette viscometer and a capillary viscometer; (b) time evolution of primary and satellite drop positions for a pigment suspension jetted into air based on image analysis (Wang *et al.*, 2012); (c) primary and satellite drop positions as referred to in (b)

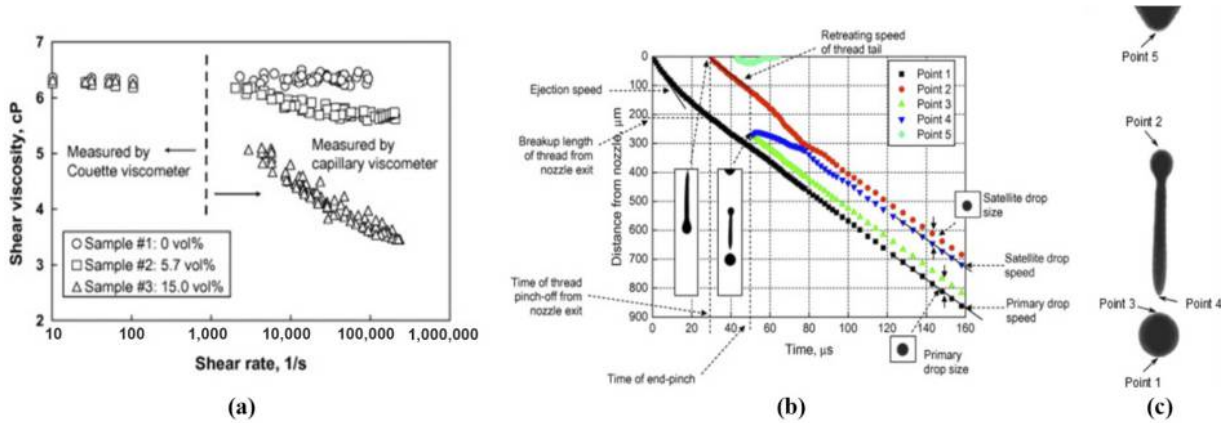

Source: Reprinted with permission from Elsevier

"satellite drops", as shown in Figure 6(a), for example. Satellite drops are small (micrometer) drops formed as the elongated filament between two adjacent drops undergoes Plateau-Rayleigh instability. At high particle concentrations, the thread formed a "spindle" structure during necking [Figure 6(b)]. The authors observed that increasing the particle concentration reduced the number of satellite drops, but the drop volumes of any satellite drops increased. They generalized the thinning of the liquid thread as a two-stage process. Long before the rupture of the liquid thread, the added particles increased the viscosity and consequently slowed down the thinning process. As the point of rupture was approached, the thinning became less consistent due to the local trapping of particles (Furbank and Morris, 2007). Similar observations have been reported by Ma *et al.* for carbon nanotube suspensions, where liquid threads containing aggregates of carbon nanotubes tended to break randomly and at an earlier time compared to liquid threads containing no carbon nanotubes (Ma *et al.*, 2008).

Mcllroy and Harlen presented a two-stage theoretical model for the capillary thinning of particle suspensions (McIlroy and Harlen, 2014). In their model, the thinning of a liquid filament was delayed initially due to the presence of particles and an increase in the bulk viscosity. As the diameter of the liquid filament reduced to about five times that of the particle diameter, thinning was accelerated due to fluctuations in local particle density. More recently, Mathues *et al.* (2015) suggested four jetting regimes during the capillary thinning of particles suspended within a Newtonian fluid. The suspension was initially considered as homogeneous viscous fluid (Regime 1) until the filament thinned to a transition radius R_T which corresponded to the onset of the concentration fluctuation regime (Regime 2). In this regime, the diluted zones thinned faster due to the local decrease in viscosity. The filament further developed into a particle-free section where the subsequent breakup followed a filament stretching process (Regime 3). The thinning rate reached maximum at this stage before it reached a deceleration regime (Regime 4). In Regime 4, the thinning followed the viscous scaling factor of the medium and showed no influence by the presence of particles.

Figure 6 (a) The time evolution of a drop containing 5 per cent (v/v) poly(methyl methacrylate) (PMMA) particles suspended in a mixture of 23 per cent (w/w) zinc chloride/water solution and UCON 90,000 (polyalkylene glycol; Dow Chemical). The images are not uniformly spaced in time; (b) this shows the drop breakup for 15, 20 and 25 per cent PMMA suspensions, respectively, where the particles may be trapped within the liquid thread during necking, forming a spindle-like structure (Furbank and Morris, 2004)

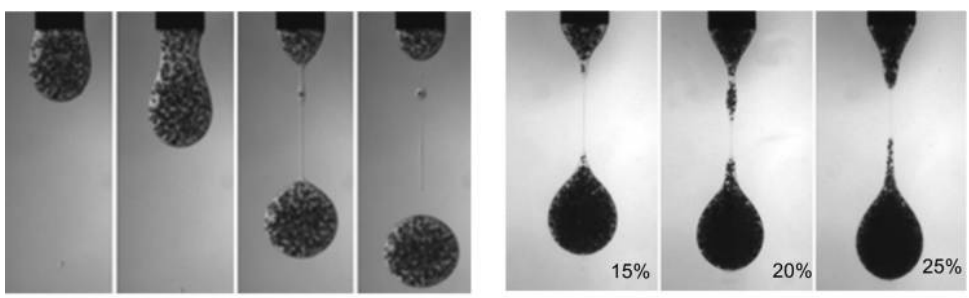

Source: Reprinted with permission from AIP Publishing LLC

Rapid Prototyping Journal
Volume 23 · Number 3 · 2017 · 562–576

4.2 Shear thinning fluids

Shear thinning fluids have been reported to suppress the formation of satellite drops that are generally considered to be undesirable in inkjet printing. Hoath *et al.* (2012) studied the effect of shear thinning on satellite drop formation using PEDOT:PSS solutions. These solutions exhibited a strong shear-thinning behavior (Figure 7). Jetting was possible because the solution experienced high shear rates and shear thinned within the print head. As soon as the drop was detached from the nozzle, the shear rate decreased and the viscosity increased, suppressing satellite drop formation. However, for highly shear-thinning fluids, any fluctuations in the shear rate within the nozzle may also lead to inconsistent jetting as the viscosity becomes highly sensitive to the shear rate. Morrison and Harlen (2011) simulated the jetting of non-Newtonian fluids using a Lagrangian finite element method. Their simulation results confirmed that shear thinning suppressed the number of satellite drops.

4.3 Viscoelastic fluids

In addition to shear-rate-dependent viscosity, inkjet fluids may exhibit elasticity when they are subjected to deformation. The elasticity may originate from the Brownian motion of small particles and/or the inclusion of polymers that are used to stabilize the particles. The viscoelastic response of the inks depends on the deformation time scale. In piezoelectric inkjet printing, the inks typically experience deformations at a frequency on the order of 10 kHz, which is not readily accessible using commercial rheometer as discussed previously. Vadillo *et al.* (2011) prepared four polymer solutions using polystyrene (PS) with different molecular weights, ranging from 110 to 488 kg/mol, and different concentrations (0-0.5 per cent). These solutions have matching linear viscoelastic data, but displayed significantly different jetting behavior, suggesting the importance of non-linear viscoelasticity in inkjet printing. In an earlier paper, the same research group correlated the inkjet printing behavior with experimental data collected from imaging the thinning process of a liquid filament formed between two pistons (Vadillo *et al.*, 2010). Recent work by Hoath *et al.* (2012) on a weak elastic polymer solution suggested that the break-off time delayed significantly as the molecular weight of the polymer increased.

4.4 Phase-changing inks and three-dimensional printing

Inkjet printing is effective in creating arbitrary planar patterns, but creating 3D objects proves to be difficult as the ink usually contains a substantial amount of solvent, which will eventually evaporate, leaving behind only a small amount of solid material (Wang *et al.*, 2008). Further, overprinting layers to create 3D structure demands a high degree of deposition precision. Such challenge can, however, be overcome by selecting a phase-change ink with little or no solvent, where the phase change is triggered chemically or thermally. Notable examples include photo-curable acrylics and wax, where additional time scales associated with the chemical reaction and heat transfer are involved. For reactive systems, premixing reactive components before printing may risk clogging the print head and inconsistent jetting as the reaction progresses soon after the mixing. To overcome this, phase change may be induced thermally or photochemically after printing. If multiple reactive components are printed onto the substrate separately, drop positioning and subsequent mixing of drops are critical. Castrejón-Pita *et al.* studied the coalescence and mixing of a sessile drop and an incoming drop. No noticeable mixing was observed when the sessile drop and the incoming drop were comparable in size. Mixing was only achieved when the sessile drop was significantly larger than the incoming drop and a vortex ring is generated (Castrejón-Pita *et al.*, 2013). The inkjet printing of reactive materials has been successfully applied to pattern polymers, metals, quantum dots, biomaterials, etc. (Delaney *et al.*, 2010; Kim *et al.*, 2013; Kramb *et al.*, 2014; Wang *et al.*, 2008). Fathi and Dickens (2012) studied the drop formation instability of caprolactam mixtures and suggested the possibility of building 3D structures layer by layer through inkjet printing two reactive components sequentially, followed by polymerization (Figure 8).

3D printing is one of the fastest growing technologies in recent years, although the original concept of rapid prototyping was conceived much earlier. Certain types of 3D

Figure 7 (a) Shear viscosity data of different concentrations of PEDOT:PSS in water; (b) jetting of 1 per cent (w/w) aqueous PEDOT:PSS solution and 60 per cent (w/w) glycerol in water, respectively

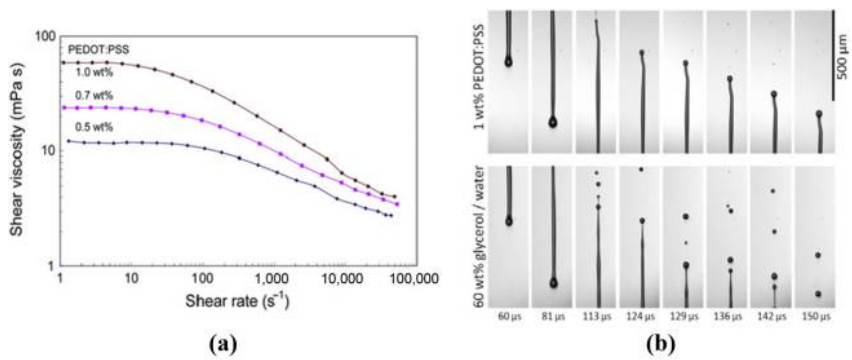

Note: The PEDOT:PSS solution showed fewer satellite drops relative to the glycerol solution (Hoath *et al.*, 2012)
Source: Reprinted with permission from Elsevier

Figure 8 Proposed method of creating nylon on a substrate by inkjet printing Mixture A (caprolactam and the catalyst) followed by Mixture B (caprolactam and a catalyst activator). The mixture of A and B was then heated by radiation to form nylon (Fathi and Dickens, 2012)

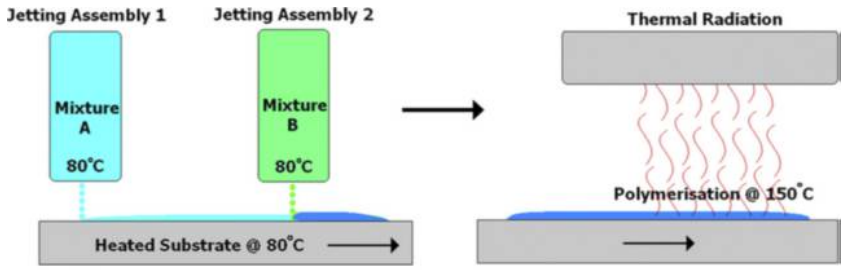

Source: Reprinted with permission from ASME publishing group

printing technology are based on inkjet technology and can be traced back to 1994. Gao and Sonin (1994) from MIT described a method for the fabrication of 3D structures by printing wax microdrops. The wax droplets solidify upon contacting the substrate maintained at a lower temperature. It is worth noting that heat transfer is generally faster than mass transfer processes, meaning that there is little or no further movement upon deposition. Wax also has the additional advantage of offering long-term stability for printing materials containing particles. The particles embedded within the wax will have no mobility until the wax is heated up immediately prior to printing. Some 3D printing methods use wax as a support material which will be removed after the parts are completed. Another type of 3D printing methods involves inkjet printing a binder solution (e.g. gypsum, water and organic solvents) onto a powder bed to consolidate the powder. However, using a solvent as the binder tends to create parts with pores, limiting the mechanical and dielectric properties. To create parts that are relatively pore-free, Wang *et al.* (2008) inkjet printed a photo-curable resin onto a powder bed instead. The wetting of drops on the powder bed is crucial and will be discussed in the next section.

4.5 Bio-printing

3D printing using biological cells as the building blocks opens up new exciting opportunities in regenerative medicine and drug screening. It also enables the creation of cell culture models for studying cellular communications and disease progression (Khetan and Burdick, 2011). Many studies suggested that although cells may be damaged during the printing, cell viability is not significantly reduced with special precautions (Calvert, 2007; Lorber *et al.*, 2014; Murphy and Atala, 2014; Saunders *et al.*, 2008; Xu *et al.*, 2005). Further, most existing studies on bioprinting focus on the correlation between printing conditions and cell viability, and relatively few studies directly address how the inclusion of cells impacts the drop formation process in inkjet printing. Xu *et al.* studied the drop formation of a "bio-ink" suspension containing cells and sodium alginate (NaAlg) in terms of drop detachment time, drop volume, drop velocity and the number of satellite drops (Figure 9) (Xu *et al.*, 2014). It was observed that as the cell concentration increased, the droplet size and velocity decreased, whereas the breakup time became longer with fewer or no satellite drops.

5. Drop impact, footprint and resolution

5.1 Contact angle

In inkjet printing, the final footprint, or contact diameter, of a drop upon deposition onto a substrate is determined by the in-flight drop diameter (d_0) as well as the contact angle – the angle between the liquid/vapor interface and the solid substrate. The drop footprint in turn determines the spatial resolution of the inkjet printing. If in-flight solvent evaporation is neglected, the final footprint (d_{con}) of the drop can be estimated from mass balance (Derby, 2010):

$$d_{con} = d_0^3 \sqrt{\frac{8}{\tan(\theta_{eqm}/2)(3 + \tan^2(\theta_{eqm}/2))}} \quad (2)$$

where θ_{eqm} is the equilibrium contact angle.

Equation (2) predicts that a 1-picoliter droplet will give a final "footprint" of ca. 30 μm for a contact angle of 10°. To obtain a footprint smaller than the in-flight drop size, equation (2) estimates that an equilibrium contact angle larger than approximately 110° is needed. Such simple calculations offer a rough guidance on the type of contact angle required, but clearly do not consider the surface roughness or porosity of the substrate; the rheology and dynamics involved (e.g.

Figure 9 Schematic diagram of an experimental setup for inkjet printing a "bioink" – an aqueous suspension of cells and NaAlg. The inset figures show the excitation waveform and the drop formation of a bioink containing 1×10^7 cells/ml (Xu *et al.*, 2014)

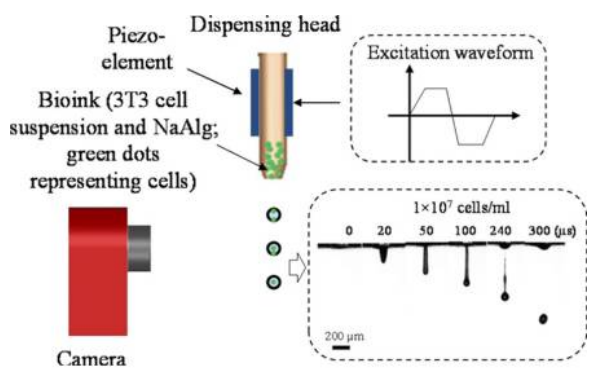

Source: Reprinted with the permission of the American Chemical Society

bouncing of the drops after initial impact); and possible "coffee-ring" effect, where the higher solvent evaporation rate at the edge of the droplet leads to particle deposition at the edge, pinning down the contact line (Deegan *et al.*, 1997). In general, a number of events, such as capillary spreading, retraction and oscillation, usually occur before the solidification of the droplet. In addition to the previously discussed Re, We and Oh numbers, the dynamic advancing and receding contact angles are also important, as they are related to the spreading and recoiling of the drop upon impact. Hsiao *et al.* (2014) reported that the maximum drop spreading radii were significantly underestimated without considering the impact initial. The drop impact on relatively smooth and flat surfaces has been intensely studied by Derby (2010), and an excellent review on this topic has been given by Yarin (2006). The interactions between multiple drops during the deposition of inkjet printing has been explored using simulation (Zhou *et al.*, 2015). Industrial-scale inkjet printers typically produce a line-width of 20 μm or larger, although smaller features [down to $\approx$ 100 nm (Sele *et al.*, 2005)] have been obtained via electrohydrodynamic printing, which uses an electric field to stretch the fluid (Park *et al.*, 2007), modifying the surface topology (Hendriks *et al.*, 2008) and creating a surface-energy pattern on the substrate (Sirringhaus *et al.*, 2000; Wang *et al.*, 2004).

5.2 Drop impact on rough surfaces

The apparent contact angle of a drop on the substrate depends not only on the chemical composition but also on the topology or surface roughness. The latter also forms the working principle for creating superhydrophobic surfaces (Roach *et al.*, 2008). In this review paper, we focus on the current understanding of drop impact on both porous and rough surfaces, such as those found in textiles and powder beds that are of relevance to creating conformable, stretchable electronics and 3D objects.

5.2.1 Drop impact on powder and three-dimensional printed structures

In powder-bed 3D printing, small drops (approximately 30 pl) are first generated from a binder solution. These drops then impact the powder layer at a speed on the order of 5 m/s, resulting in a crater-like structure upon impact. Increasing the drop velocity is desirable for increasing the production rate, but it also increases the impact diameter, reducing the spatial resolution. There is also a competition between the drop spreading on the surface and infiltration into the porous bed. The latter is driven by capillary forces as a result of the voids between the powder particles. To reduce powder movement upon high-velocity drop impact, a small amount of moisture may be introduced to hold the powder in place through capillary forces (Sachs *et al.*, 1993). Alternatively, the powder bed may be prepared by first spreading the powder as a wet paste, then dried to form a denser powder bed, before a binder is inkjet printed onto the bed (Grau, 1998).

Holman *et al.* (2002) studied drops that are relevant to inkjet printing and found that the infiltration time is on the order of 100-500 ms, significantly longer than the time associated with surface spreading. The authors concluded that simple models which do not consider infiltration are suffice to calculate the drop spreading even in the case of porous surfaces. Zhou *et al.* studied inkjet printing of conductive traces onto 3D printed structures created by FDM to produce embedded electronics. Their studies suggested the irregular surface of the 3D printed substrate led to discontinuity of the inkjet printed pattern and consequently poor conductivity. To improve the continuity of the inkjet printed tracks, they explored two methods: by applying heat and pressure to "iron" the surface and by using a heated metal tip to "plow" a channel to contain the ink (Zhou *et al.*, 2016).

5.2.2 Drop impact on textile surfaces

The physics of printing on textiles is rather complex because of the inherent multi-scale morphology, ranging from the filaments, yarns and weaves, to folds and wrinkles. The microstructure of non-woven textiles is rather similar to papers consists of cellulose fibers. Karaguzel *et al.* studied the jetting of microdroplets (approximately 90 μm in diameter) on nonwoven fabrics. They found that the spreading and penetration of droplets depended on the solid volume fraction (SVF) of the substrate (Karaguzel *et al.*, 2008). In the case of low-SVF, the spreading was determined by the local spacing and fiber orientation because fiber–fiber distance is much larger than the drop diameter. For high-SVF, the spreading and penetration of drops are more dependent on the hydrophilicity of the fiber.

More recently, Park *et al.* (2006) systematically studied the correlations between different types of woven structures and the corresponding drop spreading. They observed that the printing qualities (line width, edge sharpness, etc.) depended on the fabric structural parameters, surface chemistry and the ink. As shown in Figure 10, when the print direction is parallel to the warp direction, wicking occurs perpendicular to the print direction, increasing the actual line width and consequently lowering the print resolution. Conversely, the actual line width is closer to the minimum or target line width when the print direction is perpendicular to the warp direction. Several studies pointed out that drop splashing on rough surface becomes more prominent as the ratio of surface roughness to the drop size increases (Shakeri and Chandra, 2002; Šikalo *et al.*, 2005; Sivakumar *et al.*, 2005). Parallel grove structures have been created by Kannan and Sivakumar and used as a model system to understand drop impact on non-flat surfaces. The authors concluded that although both drop impact and retraction are influenced by the "surface roughness", flatness of the surface has a more pronounced effect on retraction (Kannan and Sivakumar, 2008). There are a few theoretical studies attempted to correlate the surface roughness with drop spreading and retraction (Bussmann *et al.*, 2000; Kim and Chun, 2001; Roisman *et al.*, 2002).

6. Summary and future outlook

Inkjet printing is a versatile technique capable of patterning a wide range of materials, including polymers, metals, ceramics and biomaterials. Drop formation in inkjet printing is governed by the interplay between the viscous, elastic and surface forces. The complexity of the inkjet printing lies in the multiple time scales and length scales involved. Inkjet printing is characterized by its high shear rates ($> 10^4$ s^{-1}), short residence times (5-250 μs) and high

Figure 10 (a) and (b): schematic diagrams illustrating the relationship between the actual line width and the printing direction with respect to the structure of a woven polyester fabric. In case (a), the line is printed in the warp direction, whereas in case (b), the line is printed along the filling direction. (c) and (d) are the corresponding optical micrographs of the printed lines, showing that the actual line width in case (b) is closer to the target, or minimum, line width than that in case (a) (Park *et al.*, 2006)

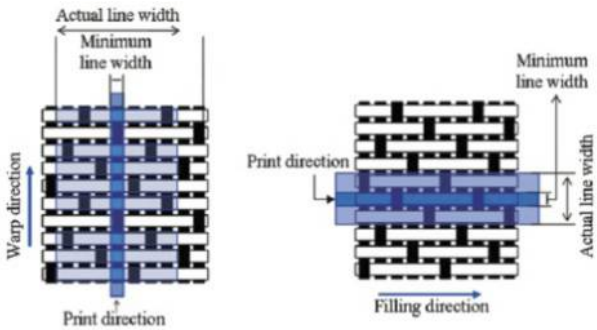

(a) Schematic of printing in warp direction

(b) Schematic of printing in filling direction

(c) Scanned image of printing in warp direction (×10)

(d) Scanned image of printing in filling direction (×10)

Source: Reprinted with permission from SAGE publications

frequencies (10-100 kHz). Jettability of Newtonian fluids has been well-studied and documented in terms of the dimensionless Ohnesorge number (Eggers and Villermaux, 2008). However, inkjet fluids may exhibit non-Newtonian behavior such as a shear-rate-dependent viscosity and viscoelasticity. In the case of inkjet printing particle suspensions, the continuum assumption breaks down as the diameter of the liquid thread decreases and becomes comparable to the size of the particles. Direct imaging of the jetting process has improved greatly with latest technological advances in high-speed and stroboscopic imaging. However, linking the jetting behavior with viscoelasticity requires assessing the rheology at high frequencies that are relevant to the inkjet printing – orders of magnitude higher than the frequency accessible by commercial rheometers. For viscoelastic fluids, additional dimensionless groups, including the Weissenberg and Deborah numbers, are used to compare the characteristic time scale of the fluid relative to the deformation time scale and time of observation. In cases where a phase-change or reactive material is used, additional time scales associated with the heat transfer and reaction also need to be considered. For biological samples, survival rate and viability of cells during and after printing are equally important to drop placement accuracy and consistency. The resolution of inkjet printing depends on the drop footprint, which is rather well-established for flat and non-porous surfaces. For applications such as electronic textiles and 3D printing, understanding drop spreading and penetration on powder beds and textiles are important for determining the lateral and depth resolution. Based on the fundamental understanding and experimental techniques as summarized in this paper, a number of topics warrant more in-depth experimental and theoretical investigations. First, as we continue to map out the operating space of inkjet printing, it is crucial to identify universal rheological fingerprints that can predict the jettability and jetting consistency. This will further translate to better quality control and faster new ink formulation and ultimately allow the rational design of printing inks based on performance as well as processability. This will be founded on the development of new, robust and affordable instruments capable of measuring fluid properties in the kHz range. Second, certain flow phenomena, such as deformation-induced thickening thixotropy, are critical to understanding inkjet, but a solid theoretical framework is still lacking (Mewis and Wagner, 2009). Thixotropy refers to the time dependency of viscosity induced by flow. Such behavior has been reported for printing inks, and it can be easily confused with viscoelastic responses (Ferna′ndez *et al.*, 1998; Liang *et al.*, 1996). Measuring and modeling thixotropy will remain an active area of research. Third, from a practical perspective, latest developments of imaging platforms (Bognet *et al.*, 2016; Castrejón-Pita *et al.*, 2008) further open up the exciting possibility of optimizing the jetting waveform in terms of the smallest drop size, drop size distribution and jetting consistency. This will further impact and guide the development of new functional inks and future print head designs. As the material set of inkjet fluids continues to expand, it becomes increasingly important to understand the underlying physics to realize the full potential of inkjet printing.

References

Adamson, A.W. (1990), *Physical Chemistry of Surfaces*, 6th ed., Wiley, New York, NY.

Bashforth, F. and Adams, J.C. (1883), *An Attempt to Test the Theories of Capillary Action by Comparing the Theoretical and Measured Forms of Drops of Fluid*, Cambridge University Press, Cambridge.

Bharathan, J. and Yang, Y. (1998), "Polymer light-emitting logos processed by ink-jet printing technology", *Proceedings of SPIE*, Vol. 3279 No. 1, pp. 78-86.

Bognet, B., Guo, Y. and Ma, A.W.K. (2016), "Controlling system components with a sound card: a versatile inkjet fluid testing platform", *Review of Scientific Instruments*, Vol. 87 No. 1, p. 015101.

Buehner, W.L., Hill, J.D., Williams, T.H. and Woods, J.W. (1977), "Application of ink jet technology to a word processing output printer", *IBM Journal of Research and Development*, Vol. 21 No. 1, pp. 2-9.

Bussmann, M., Chandra, S. and Mostaghimi, J. (2000), "Modeling the splash of a drop impacting on a solid surface", *Physics Fluids*, Vol. 12 No. 12, p. 3121.

Calvert, P. (2007), "Materials science: printing cells", *Science (New York, NY)*, Vol. 318 No. 2007, pp. 208-209.

Cappi, B., Özkol, E., Ebert, J. and Telle, R. (2008), "Direct inkjet printing of Si3N4: characterization of ink, green bodies and microstructure", *Journal of the European Ceramic Society*, Vol. 28 No. 13, pp. 2625-2628.

Castrejón-Pita, J.R., Martin, G.D., Hoath, S.D. and Hutchings, I.M. (2008), "A simple large-scale droplet generator for studies of inkjet printing", *Review of Scientific Instruments*, Vol. 79 No. 7, pp. 0-8.

Castrejón-Pita, J.R., Kubiak, K.J., Castrejón-Pita, A.A., Wilson, M.C.T. and Hutchings, I.M. (2013), "Mixing and internal dynamics of droplets impacting and coalescing on a solid surface", *Physical Review E - Statistical, Nonlinear, and Soft Matter Physics*, Vol. 88 No. 2, pp. 1-11.

Chen, H.Y., Hou, J., Zhang, S., Liang, Y., Yang, G., Yang, Y., Yu, L., Wu, Y. and Li, G. (2009), "Polymer solar cells with enhanced open-circuit voltage and efficiency", *Nature Photonics*, Nature Publishing Group, London, Vol. 3, pp. 649-653.

Clasen, C., Phillips, P.M., Palangetic, L. Vermant, J. (2012), "Dispensing of rheologically complex fluids: the map of misery", *AIChE Journal*, Vol. 58 No. 10, pp. 3242-3255.

Crowley, K., O'Malley, E., Morrin, A., Smyth, M.R. and Killard, A.J. (2008), "An aqueous ammonia sensor based on an inkjet-printed polyaniline nanoparticle-modified electrode", *The Analyst*, Vol. 133 No. 3, pp. 391-399.

de Jong, J., Jeurissen, R., Borel, H., van den Berg, M., Wijshoff, H., Reinten, H., Versluis, M., Prosperetti, A. and Lohse, D. (2006), "Entrapped air bubbles in piezo-driven inkjet printing: their effect on the droplet velocity", *Physics of Fluids*, Vol. 18 No. 12, pp. 1-7.

Dealy, J.M. (2010), "Weissenberg and Deborah numbers - their definition and use", *Bulletin of the Society of Rheology*, Vol. 79 No. 2, pp. 14-18.

Deegan, R.D., Bakajin, O., Dupont, T.F., Huber, G., Nagel, S.R. and Witten, T.A. (1997), "Capillary flow as the cause of ring stains from dried liquid drops", *Nature*, Vol. 389 No. 6653, pp. 827-829.

Delaney, J.T., Smith, P.J. and Schubert, U.S. (2009), "Inkjet printing of proteins", *Soft Matter*, Vol. 5, p. 4866.

Delaney, J.T., Liberski, A.R., Perelaer, J. and Schubert, U.S. (2010), "Reactive inkjet printing of calcium alginate hydrogel porogens – a new strategy to open-pore structured matrices with controlled geometry", *Soft Matter*, Vol. 6, p. 866.

Derby, B. (2010), "Inkjet printing of functional and structural materials: fluid property requirements, feature stability, and resolution", *Annual Review of Materials Research*, Vol. 40 No. 1, pp. 395-414.

Derby, B. (2011), "Inkjet printing ceramics: from drops to solid", *Journal of the European Ceramic Society*, Vol. 31 No. 14, pp. 2543-2550.

Dimitrov, D., Schreve, K. and Beer, N. De. (2006), "Advances in three dimensional printing - state of the art and future perspectives", *Rapid Prototyping Journal*, Vol. 12 No. 3, pp. 136-147.

Dong, H., Carr, W.W. and Morris, J.F. (2006), "Visualization of drop-on-demand inkjet: drop formation and deposition", *Review of Scientific Instruments*, Vol. 77 No. 8, p. 085101.

Dua, V., Surwade, S.P., Ammu, S., Agnihotra, S.R., Jain, S., Roberts, K.E., Park, S., Ruoff, R.S. and Manohar, S.K. (2010), "All-organic vapor sensor using inkjet-printed reduced graphene oxide", *Angewandte Chemie - International Edition*, Vol. 49 No. 12, pp. 2154-2157.

Eggers, J. and Villermaux, E. (2008), "Physics of liquid jets", *Reports on Progress in Physics*, Vol. 71 No. 3, p. 036601.

Einstein, A. (1906), "A new determination of molecular dimensions", *Annals of Physics*, Vol. 19, pp. 371-381.

Einstein, A. (1911), "A new determination of molecular dimensions", *Annalen Der Physik*, Vol. 34, pp. 591-592.

Elmqvist, R. (1951), "Measuring instrument of the recording type", US patent, 2566443.

Espalin, D., Alberto Ramirez, J., Medina, F., Johnson, W.M., Rowell, M., Deason, B. and Eubanks, M. (2014), "A review of melt extrusion additive manufacturing processes: I, process design and modeling", *Rapid Prototyping Journal Rapid Prototyping Journal Rapid Prototyping Journal Iss Rapid Prototyping Journal*, Vol. 20 No. 3, pp. 192-204.

Fathi, S. and Dickens, P. (2012), "Nozzle wetting and instabilities during droplet formation of molten nylon materials in an inkjet print head", *Journal of Manufacturing Science and Engineering*, Vol. 134 No. 4, p. 041008.

Fernández, M., Munõz, M.E., Santamaría, A., Azaldegui, R., Díez, R. and Peláez, M. (1998), "Rheological analysis of highly pigmented inks: Flocculation at high temperatures", *Journal of Rheology*, Vol. 42 No. 2, p. 239.

Fritz, G., Pechhold, W., Willenbacher, N. and Wagner, N.J. (2003), "Characterizing complex fluids with high frequency rheology using torsional resonators at multiple frequencies", *Journal of Rheology*, Vol. 47 No. 2, pp. 303-319.

Furbank, R.J. and Morris, J.F. (2004), "An experimental study of particle effects on drop formation", *Physics of Fluids*, Vol. 16 No. 5, pp. 1777-1790.

Furbank, R.J. and Morris, J.F. (2007), "Pendant drop thread dynamics of particle-laden liquids", *International Journal of Multiphase Flow*, Vol. 33 No. 4, pp. 448-468.

Gao, F. and Sonin, A.A. (1994), "Precise deposition of molten microdrops: the physics of digital microfabrication", *Proceedings of the Royal Society A: Mathematical, Physical and Engineering Sciences*, Vol. 444 No. 1922, pp. 533-554.

Gelbart, W.M. and Ben-Shaul, A. (1996), "The 'New' science of 'complex fluids'", *The Journal of Physical Chemistry*, Vol. 100 No. 31, pp. 13169-13189.

Gibson, I., Rosen, D. and Stucker, B. (2015), *Additive Manufacturing Technologies*, Springer, New York, New York, NY, available at: http://doi.org/10.1007/978-1-4939-2113-3

Grau, J.E. (1998), *Fabrication of Engineered Ceramic Components by the Slurry-Based Three Dimensional Printing Process*, MA Institute of Technology, MA.

Hendriks, C.E., Smith, P.J., Perelaer, J., Van Den Berg, A.M.J. and Schubert, U.S. (2008), "'Invisible' silver tracks produced by combining hot-embossing and inkjet printing", *Advanced Functional Materials*, Vol. 18 No. 7, pp. 1031-1038.

Hoath, S.D., Jung, S., Hsiao, W.K. and Hutchings, I.M. (2012), "How PEDOT:PSS solutions produce satellite-free inkjets", *Organic Electronics*, Vol. 13 No. 12, pp. 3259-3262.

Hoath, S.D., Vadillo, D.C., Harlen, O.G., McIlroy, C., Morrison, N.F., Hsiao, W.K., Tuladhar, T.R., Jung, S., Martin, G.D. and Hutchings, I.M. (2014), "Inkjet printing of weakly elastic polymer solutions", *Journal of Non-Newtonian Fluid Mechanics*, Vol. 205, pp. 1-10.

Hoath, S.D., Hsiao, W.K., Martin, G.D., Jung, S., Butler, S.A., Morrison, N.F., Harlen, O.G., Yang, L.S., Baine, C.D. and Hutchings, I.M. (2015), "Oscillations of aqueous PEDOT:PSS fluid droplets and the properties of complex fluids in drop-on-demand inkjet printing", *Journal of Non-Newtonian Fluid Mechanics*, Vol. 223, pp. 28-36.

Holman, R.K., Cima, M.J., Uhland, S.A. and Sachs, E. (2002), "Spreading and infiltration of inkjet-printed polymer solution droplets on a porous substrate", *Journal of Colloid and Interface Science*, Vol. 249 No. 2, pp. 432-440.

Hsiao, W.K., Martin, G.D. and Hutchings, I.M. (2014), "Printing stable liquid tracks on a surface with finite receding contact angle", *Langmuir*, Vol. 30 No. 41, pp. 12447-12455.

Hutching, I.M., Martin, G.D. and Hoath, S.D. (2007), "High speed imaging and analysis of jet and drop formation", *Journal of Imaging Science and Technology*, Vol. 51 No. 5, pp. 438-444.

Hutchings, I.M. and Martin, G.D. (2012), *Inkjet Technology for Digital Fabrication*, Wiley, Chicester.

Jang, D., Kim, D. and Moon, J. (2009), "Influence of fluid physical properties on ink-jet printability", *Langmuir*, Vol. 25 No. 5, pp. 2629-2635.

Kannan, R. and Sivakumar, D. (2008), "Impact of liquid drops on a rough surface comprising microgrooves", *Experiments in Fluids*, Vol. 44 No. 6, pp. 927-938.

Karaguzel, B., Tafreshi, H.V. and Pourdeyhimi, B. (2008), "Potentials and challenges in jetting microdroplets onto nonwoven fabrics", *Journal of the Textile Institute*, Vol. 99 No. 6, pp. 581-589.

Katstra, W., Palazzolo, R., Rowe, C., Giritlioglu, B., Teung, P. and Cima, M. (2000), "Oral dosage forms fabricated by three dimensional printing^{TM}", *Journal of Controlled Release*, Vol. 66 No. 1, pp. 1-9.

Khetan, S. and Burdick, J.A. (2011), "Patterning hydrogels in three dimensions towards controlling cellular interactions", *Soft Matter*, Vol. 7 No. 3, p. 830.

Kim, H.Y. and Chun, J.H. (2001), "The recoiling of liquid droplets upon collision with solid surfaces", *Physics of Fluids*, Vol. 13 No. 3, pp. 643-659.

Kim, K., Ahn, S. II and Choi, K.C. (2013), "Direct fabrication of copper patterns by reactive inkjet printing", *Current Applied Physics*, Vol. 13 No. 9, pp. 1870-1873.

Kirschenmann, L. and Pechhold, W. (2002), "Piezoelectric Rotary Vibrator (PRV) – a new oscillating rheometer for linear viscoelasticity", *Rheologica Acta*, Vol. 41 No. 4, pp. 362-368.

Kramb, R.C., Buskohl, P.R., Slone, C., Smith, M.L. and Vaia, R.A. (2014), "Autonomic composite hydrogels by reactive printing: materials and oscillatory response", *Soft Matter*, Vol. 10 No. 9, pp. 1329-1336.

Lamb, H. (1895), *Hydrodynamics*, University Press, Cambridge.

Larson, R.G. (1999), *The Structure and Rheology of Complex Fluids*, Oxford University Press, New York, NY.

Lean, M.H. (2002), "Method and aparatus for reducing drop placement error in printers", US patent 6367909 B1.

Leoni, N.J. and Gila, O. (2013), "Inkjet printhead and printing system with boundary layer control", US patent, 8596742 B2.

Liang, T.X., Sun, W.Z., Wang, L.D., Wang, Y.H. and Li, H.D. (1996), "Effect of surface energies on screen printing resolution", *IEEE Transactions on Components, Packaging, and Manufacturing Technology: Part B*, Vol. 19 No. 2, pp. 423-426.

Lorber, B., Hsiao, W.K., Hutchings, I.M. and Martin, K.R. (2014), "Adult rat retinal ganglion cells and glia can be printed by piezoelectric inkjet printing", *Biofabrication*, Vol. 6 No. 1, p. 015001.

McIlroy, C. and Harlen, O.G. (2014), "Modelling capillary break-up of particulate suspensions", *Physics of Fluids*, Vol. 26 No. 3, p. 033101.

McKinley, G. (2005), "Dimensionless groups for understanding free surface flows of complex fluids", *Bulletin of the Society of Rheology*, Vol. 74 No. 2, pp. 6-9.

Ma, A.W.K., Chinesta, F., Tuladhar, T. and Mackley, M.R. (2008), "Filament stretching of carbon nanotube suspensions", *Rheologica Acta*, Vol. 47 No. 4, pp. 447-457.

Martin, G.D., Hoath, S.D. and Hutchings, I.M. (2008), "Inkjet printing – the physics of manipulating liquid jets and drops", *Journal of Physics: Conference Series*, Vol. 105 No. 1, p. 012001.

Mason, W.P. (1947), "Measurement of the viscosity and shear elasticity of liquids by means of a torsionally vibrating crystal", *Transactions Of ASME*, Vol. 68, pp. 359-370.

Mathues, W., McIlroy, C., Harlen, O.G. and Clasen, C. (2015), "Capillary breakup of suspensions near pinch-off", *Physics of Fluids*, Vol. 27 No. 9, p. 093301.

Maze, C.C. and Burnet, G. (1971), "Modification of a non-linear regression technique used to calculate surface tension from sessile drops", *Surface Science*, Vol. 24 No. 1, pp. 335-342.

Melchels, F.P.W., Feijen, J. and Grijpma, D.W. (2010), "A review on stereolithography and its applications in biomedical engineering", *Biomaterials*, Vol. 31 No. 24, pp. 6121-6130.

Mewis, J. and Wagner, N.J. (2009), "Thixotropy", *Advances in Colloid and Interface Science*, Vols 147/148 No. 3, pp. 214-227.

Morita, N., Hirakata, S. and Hamazaki, T. (2010), "Study on vibration behavior of jetted ink droplets and nozzle clogging", *NIHON GAZO GAKKAISHI (Journal of the Imaging Society of Japan)*, Vol. 49 No. 1, pp. 14-19.

Morrison, N.F. and Harlen, O.G. (2011), "Inkjet printing of non-Newtonian fluids", *Proceedings 27th International Conference on Digital Printing Technologies*, *Minneapolis*, pp. 360-364.

Murphy, S.V. and Atala, A. (2014), "3D bioprinting of tissues and organs", *Nature Biotechnology*, Vol. 32 No. 8, pp. 773-785.

Okamoto, T., Suzuki, T. and Yamamoto, N. (2000), "Microarray fabrication with covalent attachment of DNA

using bubble jet technology", *Nature Biotechnology*, Vol. 18 No. 4, pp. 438-441.

Park, H., Carr, W.W., Ok, H. and Park, S. (2006), "Image quality of inkjet printing on polyester fabrics", *Textile Research Journal*, Vol. 76 No. 9, pp. 720-728.

Park, J.U., Hardy, M., Kang, S.J., Barton, K., Mukhopadhyay, D.K., Lee, C.Y., Strano, M.S., Alleyne, A.G., Georgiadis, J.G., Ferreira, P.M. and Rogers, J.A. (2007), "High-resolution electrohydrodynamic jet printing", *Nature Materials*, Vol. 6, pp. 782-789.

Perelaer, J., De Gans, B.J. and Schubert, U.S. (2006), "Ink-jet printing and microwave sintering of conductive silver tracks", *Advanced Materials*, Vol. 18 No. 16, pp. 2101-2104.

Reis, N., Ainsley, C. and Derby, B. (2005), "Ink-jet delivery of particle suspensions by piezoelectric droplet ejectors", *Journal of Applied Physics*, Vol. 97 No. 9, p. 094903.

Rida, A., Yang, L., Vyas, R. and Tentzeris, M.M. (2009), "Conductive inkjet-printed antennas on flexible low-cost paper-based substrates for RFID and WSN applications", *IEEE Antennas and Propagation Magazine*, Vol. 51 No. 3, pp. 13-23.

Riegger, L., Ernst, A. and Koltay, P. (2014), "A dispensing system for sedimenting metal microparticle solutions based on a circulation mixer method", *2nd International Conference on Micro Fluidic Handling Systems*, University of Freiburg, Germany, pp. 81-83.

Roach, P., Shirtcliffe, N.J. and Newton, M.I. (2008), "Progess in superhydrophobic surface development", *Soft Matter*, Vol. 4, p. 224.

Roisman, I.V., Rioboo, R. and Tropea, C. (2002), "Normal impact of a liquid drop on a dry surface: model for spreading and receding", *Proceedings of the Royal Society A: Mathematical, Physical and Engineering Sciences*, Vol. 458 No. 2022, pp. 1411-1430.

Rowe, C., Katstra, W., Palazzolo, R., Giritlioglu, B., Teung, P. and Cima, M. (2000), "Multimechanism oral dosage forms fabricated by three dimensional printing™", *Journal of Controlled Release*, Vol. 66 No. 1, pp. 11-17.

Sachs, E., Cima, M., Williams, P., Brancazio, D. and Cornie, J. (1992), "Three dimensional printing: rapid tooling and prototypes directly from a CAD model", *Journal of Engineering for Industry*, Vol. 114 No. 4, pp. 481-488.

Sachs, E., Allen, S., Guo, H., Banos, B., Cima, M.J., Serdy, J. and Brancazio, D. (1997), "Progress on tooling by 3D printing; conformal cooling, dimensional control, surface finish and hardness", *Proceedings of the Eighth Annual Solid Freeform Fabrication Symposium*, *Austin*, pp. 115-124.

Sachs, E., Cima, M., Cornie, J., Brancazio, D., Bredt, J., Curodeau, A., Fan, T., Khanuja, S., Laude, A., Lee, J. and Michaels, S. (1993), "Three-dimensional printing: the physics and implications of additive manufacturing", *CIRP Annals – Manufacturing Technology*, Vol. 42 No. 1, pp. 257-260.

Saunders, R.E., Gough, J.E. and Derby, B. (2008), "Delivery of human fibroblast cells by piezoelectric drop-on-demand inkjet printing", *Biomaterials*, Vol. 29 No. 2, pp. 193-203.

Seerden, K., Reis, N., Evans, J., Grant, P., Halloran, J. and Derby, B. (2001), "Ink-jet printing of wax-based alumina suspensions", *Journal of American Ceramic Society*, Vol. 84 No. 11, pp. 2514-2520.

Sele, C.W., Von Werne, T., Friend, R.H. and Sirringhaus, H. (2005), "Lithography-free, self-aligned inkjet printing with sub-hundred-nanometer resolution", *Advanced Materials*, Vol. 17 No. 8, pp. 997-1001.

Shakeri, S. and Chandra, S. (2002), "Splashing of molten tin droplets on a rough steel surface", *International Journal of Heat and Mass Transfer*, Vol. 45 No. 23, pp. 4561-4575.

Shimoda, T., Morii, K., Seki, S. and Kiguchi, H. (2003), "Inkjet printing of light-emitting polymer displays", *MRS Bulletin*, Vol. 28 No. 11, pp. 821-827.

Šikalo, Š., Wilhelm, H.D., Roisman, I.V., Jakirlić, S. and Tropea, C. (2005), "Dynamic contact angle of spreading droplets: experiments and simulations", *Physics of Fluids*, Vol. 17 No. 6, pp. 1-13.

Singh, M., Haverinen, H.M., Dhagat, P. and Jabbour, G.E. (2010), "Inkjet printing-process and its applications", *Advanced Materials*, Vol. 22 No. 6, pp. 673-685.

Sirringhaus, H., Kawas, T., Friend, R.H., Shimoda, T., Inbasekaran, M., Wu, W. and Woo, E.P. (2000), "High-resolution inkjet printing of all-polymer transistor circuits", *Science*, Vol. 290, pp. 2123-2126.

Sivakumar, D., Katagiri, K., Sato, T. and Nishiyama, H. (2005), "Spreading behavior of an impacting drop on a structured rough surface", *Physics of Fluids*, Vol. 17 No. 10, pp. 1-11.

Sweet, R.G. (1965), "High frequency recording with electrostatically deflected ink jets", *Review of Scientific Instruments*, Vol. 36 No. 2, pp. 131-136.

Sweet, R.G. (1975), "Fluid droplet recorder", US Patent 3596275.

Tortorich, R. and Choi, J.W. (2013), "Inkjet printing of carbon nanotubes", *Nanomaterials*, Vol. 3, pp. 453-468.

Turner, B.N. and Gold, S.A. (2015), "A review of melt extrusion additive manufacturing processes: II, materials, dimensional accuracy, and surface roughness", *Rapid Prototyping Journal*, Vol. 21 No. 3, pp. 250-261.

Upcraft, S. and Fletcher, R. (2003), "The rapid prototyping technologies", *Assembly Automation*, Vol. 23 No. 4, pp. 318-330.

Utela, B., Storti, D., Anderson, R. and Ganter, M. (2008), "A review of process development steps for new material systems in three dimensional printing (3DP)", *Journal of Manufacturing Processes*, Vol. 10 No. 2, pp. 96-104.

Vadillo, D.C., Hoath, S.D., Hsiao, W.K. and Mackley, M.R. (2011), "The effect of inkjet ink composition on rheology and jetting behaviour", NIP and Digital Fabrication.

Vadillo, D.C., Tuladhar, T.R., Mulji, A.C., Jung, S., Hoath, S.D. and Mackley, M.R. (2010), "Evaluation of the inkjet fluid's performance using the 'Cambridge Trimaster' filament stretch and break-up device", *Journal of Rheology*, Vol. 54 No. 2, p. 261.

van den Berg, A.M.J., Smith, P.J., Perelaer, J., Schrof, W., Koltzenburg, S. and Schubert, U.S. (2007), "Inkjet printing of polyurethane colloidal suspensions", *Soft Matter*, Vol. 3, p. 238.

Vaught, J.L., Cloutier, F.L., Donald, D.K., Meyer, J.D., Tacklind, C.A. and Taub, H.H. (1984), "Thermal ink jet printer", US patent 4490728.

Versluis, M. (2013), "High-speed imaging in fluids", *Experiments in Fluids*, Vol. 54 No. 2, p. 1458.

von Hasseln, K.W. (2013), "Apparatus and method for producing a three-dimentional food product", US Patent 0034633 A1.

Wagner, N.J. and Brady, J.F. (2009), "Shear thickening in colloidal dispersions", *Physics Today*, Vol. 62 No. 10, pp. 27-32.

Wang, T., Patel, R. and Derby, B. (2008), "Manufacture of 3-dimensional objects by reactive inkjet printing", *Soft Matter*, Vol. 4, p. 2513.

Wang, X., Carr, W.W., Bucknall, D.G. and Morris, J.F. (2012), "Drop-on-demand drop formation of colloidal suspensions", *International Journal of Multiphase Flow*, Vol. 38 No. 1, pp. 17-26.

Wang, J.Z., Zheng, Z.H., Li, H.W., Huck, W.T.S. and Sirringhaus, H. (2004), "Dewetting of conducting polymer inkjet droplets on patterned surfaces", *Nature Materials*, Vol. 3 No. 3, pp. 171-176.

Xu, T., Jin, J., Gregory, C., Hickman, J.J. and Boland, T. (2005), "Inkjet printing of viable mammalian cells", *Biomaterials*, Vol. 26 No. 1, pp. 93-99.

Xu, C., Zhang, M., Huang, Y., Ogale, A., Fu, J. and Markwald, R.R. (2014), "Study of droplet formation process during drop-on-demand inkjetting of living cell-laden bioink", *Langmuir*, Vol. 30 No. 30, pp. 9130-9138.

Yan, X. and Gu, P. (1996), "A review of rapid prototyping technology and systems", *Computer Aided Design*, Vol. 28 No. 4, pp. 307-318.

Yang, L., Rida, A., Vyas, R. and Tentzeris, M.M. (2007), "RFID tag and RF structures on a paper substrate using inkjet-printing technology", *IEEE Transactions on Microwave Theory and Techniques*, Vol. 55 No. 12, pp. 2894-2901.

Yang, L., Kazmierski, B.K., Hoath, S.D., Jung, S., Hsiao, W.K., Wang, Y., Berson, A., Harlen, O., Kapur, N. and Bain, C.D. (2014), "Determination of dynamic surface tension and viscosity of non-Newtonian fluids from drop oscillations", *Physics of Fluids*, Vol. 26 No. 11, p. 113103.

Yarin, A.L. (2006), "Drop impact dynamics: splashing, spreading, receding, bouncing. . .", *Annual Review of Fluid Mechanics*, Vol. 38, pp. 159-192.

Zhou, W., List, F.A., Duty, C.E. and Babu, S.S. (2016), "Fabrication of conductive paths on a fused deposition modeling substrate using inkjet deposition", *Rapid Prototyping Journal*, Vol. 22 No. 1, pp. 77-86.

Zhou, W., Loney, D., Fedorov, A.G., Degertekin, F.L. and Rosen, D.W. (2015), "Shape evolution of multiple interacting droplets in inkjet deposition", *Rapid Prototyping Journal*, Vol. 21 No. 4, pp. 373-385.

Corresponding author

Anson W. K. Ma can be contacted at: anson.ma@uconn.edu